AFOSR 1961

THE UNIVERSITY OF MICHIGAN

COLLEGE OF ENGINEERING

Department of Chemical and Metallurgical Engineering

Technical Note

SINTERING OF ZINC OXIDE

L. F. Norris

G. Parravano

ORA Project 02832

under contract with:

UNITED STATES AIR FORCE

AIR RESEARCH AND DEVELOPMENT COMMAND

AIR FORCE OFFICE OF SCIENTIFIC RESEARCH

CONTRACT NO. AF 49(638)-493

PROJECT NO. 9762, TASK NO. 37621

WASHINGTON, D.C.

administered through:

OFFICE OF RESEARCH ADMINISTRATION ANN ARBOR

March 1962

ABSTRACT

Sintering studies have been conducted with single-crystal spheres of zinc oxide in air and at lower oxygen partial pressures and total pressures of 10^{-3} to 1.0 atmospheres over a temperature range of 1050-1250°C. Quantitative observations on the rate of growth of a neck between the spheres were made. No change in the distance between the geometrical centers of the spheres was observed. An analysis of the kinetic data shows that sintering was predominantly achieved by distillation through the surrounding gas phase. At higher total pressures there was evidence that diffusion through a hydrodynamic boundary layer above the solid surface was the rate-controlling step, while at lower pressures sintering was determined by the rate of evaporation. Previous studies of the welding together of zinc oxide microspheres in the temperature range 700-900°C have emphasized the operation of a bulk diffusional transport process, dependent on the nonstoichiometry of zinc oxide. Additional evidence to support this conclusion was obtained in the present work. The pattern of the prevailing transport mechanisms in zinc oxide from 700 to 1250°C is analyzed, and its application to other solid-state transfer processes is discussed.

INTRODUCTION

Sintering characteristics of zinc oxide compacts are known to depend on experimental conditions like the stoichiometry of the oxide, chemical composition of the surrounding atmosphere, temperature, and purity of the oxide.[1] Variations in sintering behavior reflect the operation of different transport mechanisms underlying sintering. Previous studies of the welding together of single crystal microspheres of zinc-rich zinc oxide showed that volume diffusion is responsible for the observed sintering in the temperature range 700°-900°C, the driving force for the process being supplied by the oxidation of the excess zinc present.[2] It thus seemed of interest to investigate the extent to which this mechanism would operate under different experimental conditions, and whether the reported variations of sintering characteristics of compacts of zinc oxide also are present in the welding together of single-crystal microspheres.

The results obtained in the temperature range 1050°-1250°C point to the operation of a transport process which is distinctly different from any which predominates at lower temperatures.

EXPERIMENTAL

Sintering data were obtained by measuring the growth rate of the neck formed between two contacting microspheres of zinc oxide. The spheres were obtained by crushing clear, single crystals of zinc oxide into smaller crystals which were ground and polished using air-grinding techniques previously discussed.[2] Final diameters of the spheres were in the range of 0.5 mm. The chemical composition and X-ray and spectroscopic analysis of the zinc oxide samples, together with the average value of their electrical conductivity, has already been reported.[2]

Two or more microspheres were placed in a groove cut in a 10% rhodium-platinum rod which formed the heating element of a totally enclosed hot stage.[3] Observations were made through an optically flat quartz window. A creep-test microscope, equipped with a filar eye-piece micrometer, was vertically mounted above the heating rod, enabling measurement of the growth of the bridge between spheres. Neck width was measured directly at sintering temperatures. Measurements of the distance between a fixed number of spheres were used to check the presence of shrinkage.

The electrical circuit controlling the current to the heating rod consisted of a step-down transformer, variac, and voltage stabilizer. Temperatures were measured with a potentiometer and a Pt-Pt Rh thermocouple welded to the rod directly under the location of the zinc oxide microspheres. Tem-

peratures were kept at a constant value (± 2°C) by a stepless controller connected to a saturable reactor.

Sintering studies were made in air, helium, and in hydrogen and steam mixtures. The latter were prepared by adding hydrogen from an electrolytic cell to a known flow rate of purified helium and saturating the mixture with water vapor. Compositional equilibrium was assured by maintaining a 5°C temperature difference between two saturators through which the hydrogen-helium mixture was passed. For runs made in air a flow rate of approximately 25 cc per minute was maintained. Preliminary runs showed no effect of the flow rate on the rate of sintering within gas flow rates of from 0 to 75 cc per minute. Flow rates at sub-atmospheric pressure were obtained with a vacuum pump and capillary tubings on each side of the hot stage. Pressure was read with a mercury manometer connected to the vacuum system.

RESULTS

Typical results for sintering in air at 1 atm and temperatures of 1050-1250°C are shown in Fig. 1. The reproducibility of the data can be gauged from Fig. 2, which includes results from four runs under similar conditions. An incubation period was sometimes observed at low temperatures. During this time, no observable sintering took place. The duration of the period was less random than that observed in previous studies,[3] and there was evidence that it was largely due to the inability to resolve a neck width of less than about 0.07 mm with the microscope used.

The effect of the total gas pressure on the slope (x^3/a) deduced from typical sintering plots (Figs. 1 and 2) is shown in Fig. 3, where x and a are the diameters of the neck and of the spheres, respectively. No effect on the rate of sintering was detected when at constant total pressure and temperature, the oxygen partial pressure of the surrounding gas phase was varied from atmospheric to 6.3×10^{-4} atm.

Long, needle-shaped crystals developed on the surface of the spheres at temperatures > 1150°C. They showed no preferential region of growth on the spheres. At 1250°C crystallite formation posed experimental difficulties by growing across the neck region and obscuring observation. Sometimes a crystallite bridge, produced by interlocking crystallites, was formed before substantial sintering occurred. These facts are reminiscent of similar observations on vanadium pentoxide spheres. In this instance, it was shown that whisker growth between adjacent spheres was the first stage of the sintering process between two spheres of vanadium pentoxide.[4]

Measurements of end-to-end distances for two sintering spheres in air generally showed no change during sintering. Occasionally an increase in the end-to-end distance was observed. Metallographic examination of spheres exhibiting this

behavior revealed the presence of a whisker embedded in the neck region. The whisker, growing from one sphere, had evidently moved the other sphere until friction with the heating groove halted the motion and allowed the subsequent welding process.

DISCUSSION

The most significant conclusions which can be derived from the experimental data presented in the previous section are as follows:

(a) Neck growth between single-crystal zinc oxide micro-spheres occurred readily in the temperature range 1050° to 1250°C.

(b) At constant temperature and pressure, the experimental results could be fitted into an equation

$$x^m = kt \qquad (1)$$

(Fig. 1), the average value of m being 3. This value was obtained by averaging the results of about 40 runs, whose maximum deviation never exceeded ± 0.6. There was a tendency, however, for m to decrease as the temperature decreased.

(c) At constant temperature, the rate of neck growth was not affected by the oxygen partial pressure of the surrounding atmosphere.

(d) At constant temperature, the rate of neck growth was only slightly dependent on the total pressure, except at higher pressures. In this range the rate was adversely affected by the total pressure (Fig. 3).

(e) The rate of neck growth varied exponentially with temperature. The temperature coefficient of the rate was not dependent on the total pressure.

(f) Over the whole range of experimental conditions investigated, the rate was independent of the flow velocity of the carrier gas.

According to previous derivations,[5] results under (b) indicate that the rate of growth of the neck was controlled by distillation of matter from the sphere surfaces to the neck region. Results under (c) and (d) show that the distillation process is controlled by the rate of evaporation of matter from the zinc oxide surface. At higher total pressures, diffusive effects through a boundary layer adjacent to the solid surface play an increasingly important role. Furthermore, at lower temperatures a different transport mechanism sets in. This is evidenced by the tendency for m to have values > 3.

When the rate of evaporation of the sintering spheres is the kinetically controlling factor, the rate of mass transported to the neck area is given by:[5]

$$\frac{x^3}{a} = \frac{3\pi M\gamma p}{\rho^2 RT}\left(\frac{M}{2\pi RT}\right)^{1/2} t \qquad (2)$$

where M is the molecular weight of the solid species, p the equilibrium partial pressure, ρ the density, t time, and γ the surface tension.

Comparing Eq. (2) with the empirical expression (1), one obtains m = 3. This is consistent with our findings (Fig. 1). Since nonstoichiometric zinc oxide can be regarded as a solid solution of zinc in zinc oxide, its evaporation is incongruent. Assuming that zinc oxide and zinc are the gaseous species formed, the evaporation reactions are:

$$ZnO(\text{in } Zn_xO(g)) = ZnO(g)$$

$$Zn(\text{in } Zn_xO(g)) = Zn(g)$$

where $x > 1$. In the gas phase, then, the following equilibrium is established:

$$Zn(g) + 1/2\ O_2(g) = ZnO(g)$$

Experimentally, zinc oxide seems to be the predominant gaseous species[6] and, for the purpose of our discussion, the dissociation reaction will be neglected. Equation (2) may be solved for p. Taking the value of x, averaged over several runs conducted at total pressures < 1 atm at 1150°C, ρ = 5.61 gr per cc, and γ = 1000 dynes per cm^2, it is possible to calculate a value of p = 0.082 mm Hg. This value is in satisfactory agreement with the literature value of 0.062 mm Hg.[7] In addition, numerical values for the evaporation rates can be computed from our data. Taking the neck volume equal to $\pi x^4/16a$, and assuming that all zinc oxide evaporated was condensed in the neck area from runs completed at 1150°C and 2.7×10^{-3} atm, the evaporation rate from two spheres can be found equal to 3.11×10^{-8} gr hr^{-1}. In a study of the rate of formation of zinc aluminate from zinc oxide and alumina, in the same temperature range as used in the present sintering experiments, the rate of evaporation of zinc oxide was found to be:[8]

$$R = 6.3 \times 10^9 \exp\left\{-\frac{95{,}000}{RT}\right\} \text{ gr cm}^{-1}\text{hr}^{-1} \qquad (3)$$

Under the conditions of the present experiments, Eq. (3) gives R = 8.08×10^{-7} gr per hr. This result is within an order of magnitude of the value calculated from sintering.

At total pressures close to 1 atm the rate of neck growth was influenced by the total pressure. This indicates that diffusional transport in the gas phase becomes a controlling factor of the evaporation process. Since the flow rate of the carrier gas did not influence the observed growth rate of the neck, the resistance to the flux of evaporating species can be traced to natural convection through a density gradient in the vapor of zinc oxide adjacent to the solid surface. A calculation of the evaporating flux and sintering rate under these conditions has been performed recently.[9]

Assuming a mass flow perpendicular to the surface of condensation and the Fuchs model for the evaporation and condensation, the sintering rate was found to be:

$$\frac{x^3}{a} = \frac{6\pi D}{\delta}\left[\frac{M}{\rho RT}\right]^2 \gamma p t \qquad (4)$$

where δ, D are the thickness of the surface film and the diffusion coefficient for species in the gas phase, respectively. From the value of the mean free path in the gas phase, $\delta \approx 10^{-4}$cm and D can be calculated to be ≈ 2.0 cm^2 per sec.[10] Using these values in Eq. (4) and our experimental data for runs at 1 atm and 1150°C, a value of $p_x = 0.093$ mm Hg is deduced. This value is again in good agreement with that obtained by direct measurements quoted above.[7] It should be noted that no agreement in the value of the equilibrium vapor pressure obtains for runs at 1 atm if the model based on the rate of evaporation as controlling step is used.

The effect of a change in size of the spheres on the sintering rate for the mechanisms discussed above shows[9,11] that in both cases the ratio between the times required for the growth of similar neck width is the following function of the sphere diameters:

$$\lambda^2 = \frac{\Delta t_1}{\Delta t_2} = \left(\frac{a_1}{a_2}\right)^2 \qquad (5)$$

Figure 4 compares values of $\left(\frac{a_1}{a_2}\right)^2$ as obtained from observed times for equivalent amounts of sintering with values obtained directly from the sphere radii ratios. Although the range of λ investigated was only 1 to 1.4, it is clear from Fig. 4 that relation (5) is satisfactorily obeyed.

The activation energy calculated from the experimental data (Fig. 5) is 105-110 k cal/mole. This result should be compared with the value of 95 k cal/mole of Eq. (3). It is also consistent with the value of the evaporation

energy of zinc oxide of 123 k cal/mole.[7] The high- and low-pressure data should yield, as was found, the same value of the activation energy for the rate of neck growth, since in the case of diffusional control of the evaporation, the only temperature-dependent factor in the final rate expression is the vapor pressure of zinc oxide. The observation that the center-to-center distance of spheres during sintering remained constant can be taken as further evidence for the operation of the distillation mechanism.

Previous studies on the sintering of zinc oxide[2] at lower temperatures (700-900°C) have emphasized the role of nonstoichiometric zinc ions in zinc oxide. It was postulated that the differences in excess zinc ion concentration between the surface and the interior of the spheres were responsible for the sintering behavior. Diffusional transfer of the excess zinc through the zinc oxide crystal and subsequent surface oxidation accounted for the increase in sphere diameter and the accompanying formation of a neck between spheres. The mechanism was supported by experimental evidence on the limited extent of sintering possible, since no further neck growth occurred after a given period. This extent is related to the initial amount of excess zinc present.

The present studies verified this sintering mechanism. Measurements made on a single sphere at 800°C revealed a diameter increase corresponding to a neck growth $x/a = 0.125$ for spheres 0.585 mm in diameter. No further increase in neck was observed after the indicated diameter change.

CONCLUSION

It is instructive to summarize briefly the results of these studies on the transport mechanisms observed during the welding together of zinc oxide single-crystal spheres. At low temperatures a solid-state diffusional transport predominates. The transport is affected by the nonstoichiometric nature of zinc oxide and involves a relatively low activation energy (~ 35 k cal/mole). There is strong evidence that the carriers are excess zinc ions. Oxygen partial pressure and impurity content of zinc oxide affect the rate of welding. Furthermore, differences in chemical potential of the zinc ions may arise either as a result of surface oxidation (chemical sintering) or as a consequence of the presence of the small convex neck area (physical sintering). In both cases the bulk of the spheres is the source of the carriers, but their sink is represented by the surface of the sphere for the former, and by the neck area for the latter case. Between 700-900°C chemical sintering is predominant, while physical sintering through bulk diffusion is appreciable at about 1000-1100°C. At still higher temperatures, the diffusional transport is greatly overshadowed by the transfer of matter through the surrounding gas phase. Sintering then becomes dependent on the rate of evaporation of zinc oxide. In principle, three cases are possible. The transport through the gas phase may not be slowed down by convective phenomena. The rate of transfer is then controlled by the rate of evaporation and is independent of total pressure

and gaseous flow rate, and it involves a rather high activation energy (109 k cal/mole). This mechanism tends to occur at lower total pressures At higher pressures, diffusive control of the rate of evaporation sets in. Sintering becomes dependent on the total pressure (natural convection) and, at high flow velocities, should be proportional to a fractional power of the flow velocity of the carrier gas (forced convection). The high-temperature mechanisms are independent of the oxygen partial pressure of the gas phase. The energy values involved in solid diffusion and evaporation are the factors which determine the type of sintering followed. Possibly the pattern of transport mechanisms emerging from these studies can be expanded to cover different substances and transport phenomena (solid-state reactions).

REFERENCES

1. Allsopp, H. J., and J. P. Roberts, Trans. Faraday Soc., 55, 1386 (1959).

2. Lee, V. J., and G. Parravano, J. Appl. Phys., 30, 1735 (1959).

3. O'Bryan, H. M., Jr., and G. Parravano, "Sintering of Titanium Dioxide," in: Powder Metallurgy, Werner Leszynski, Editor, Interscience Publishers, New York (1961).

4. Parravano, G., Gazz. Chin. Ital., 91, 467 (1961).

5. Kingery, W. D., and M. Berg, J. Appl. Phys., 26, 1205 (1955).

6. Brewer, L., Chem. Rev., 52, 1 (1953).

7. Gmelins Handbuch der Anorganischen Chemie, Zink, Verlag Chemie GMBH, Weinheim/Bergstrasse (1956).

8. Bengtson, B., and R. Jagitsch, Arkiv. Kem., Mineral Geol., 24A, No. 18 (1947).

9. Moser, J. B., and D. H. Whitmore, J. Appl. Phys., 31, 488 (1960).

10. Reid, R. C., and T. K. Sherwood, The Properties of Gases and Liquids, New York (1958).

11. Herring, C., J. Appl. Phys., 21, 301 (1950).

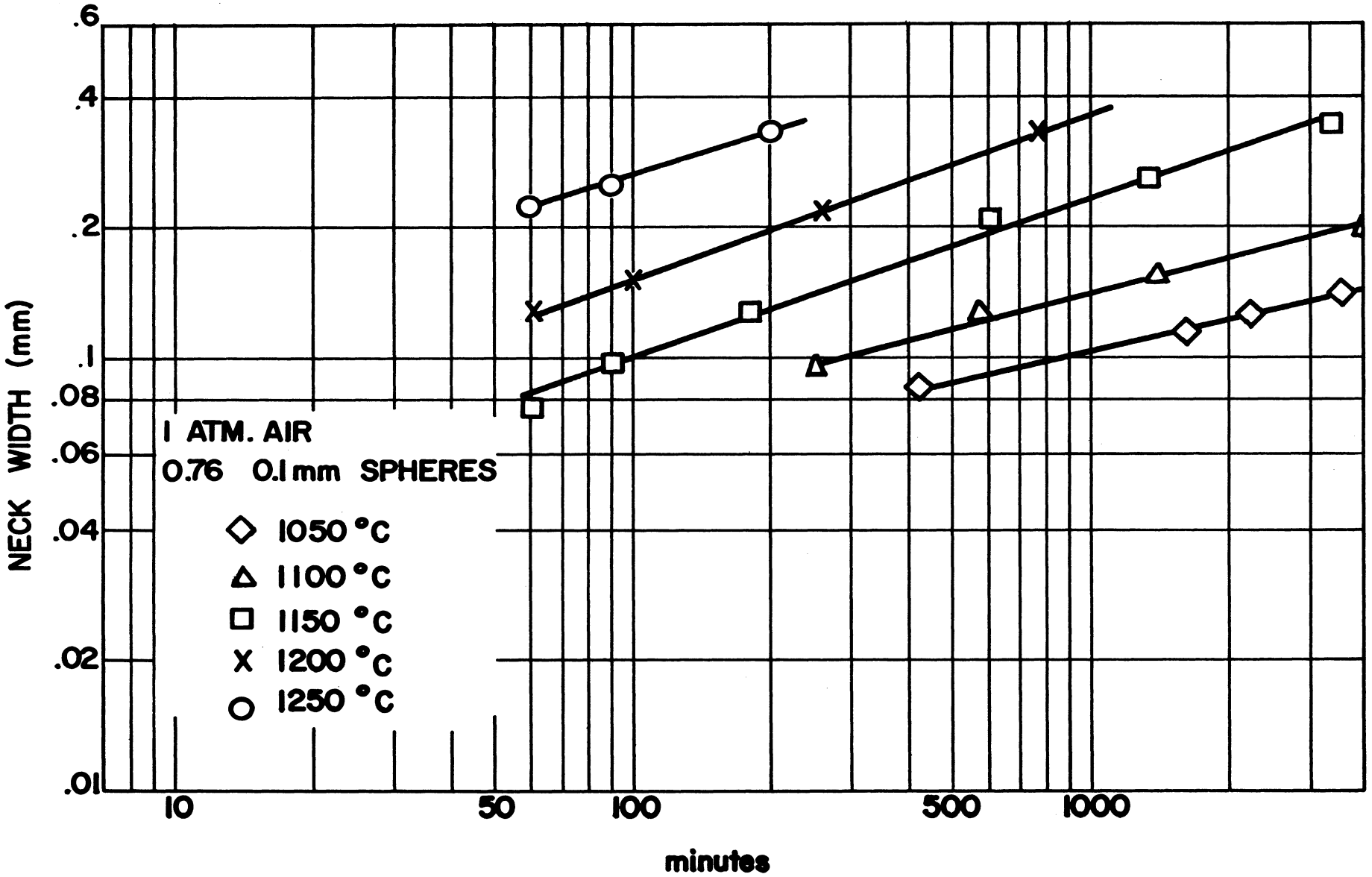

Fig. 1. Sintering of zinc oxide microspheres: neck width vs. time.

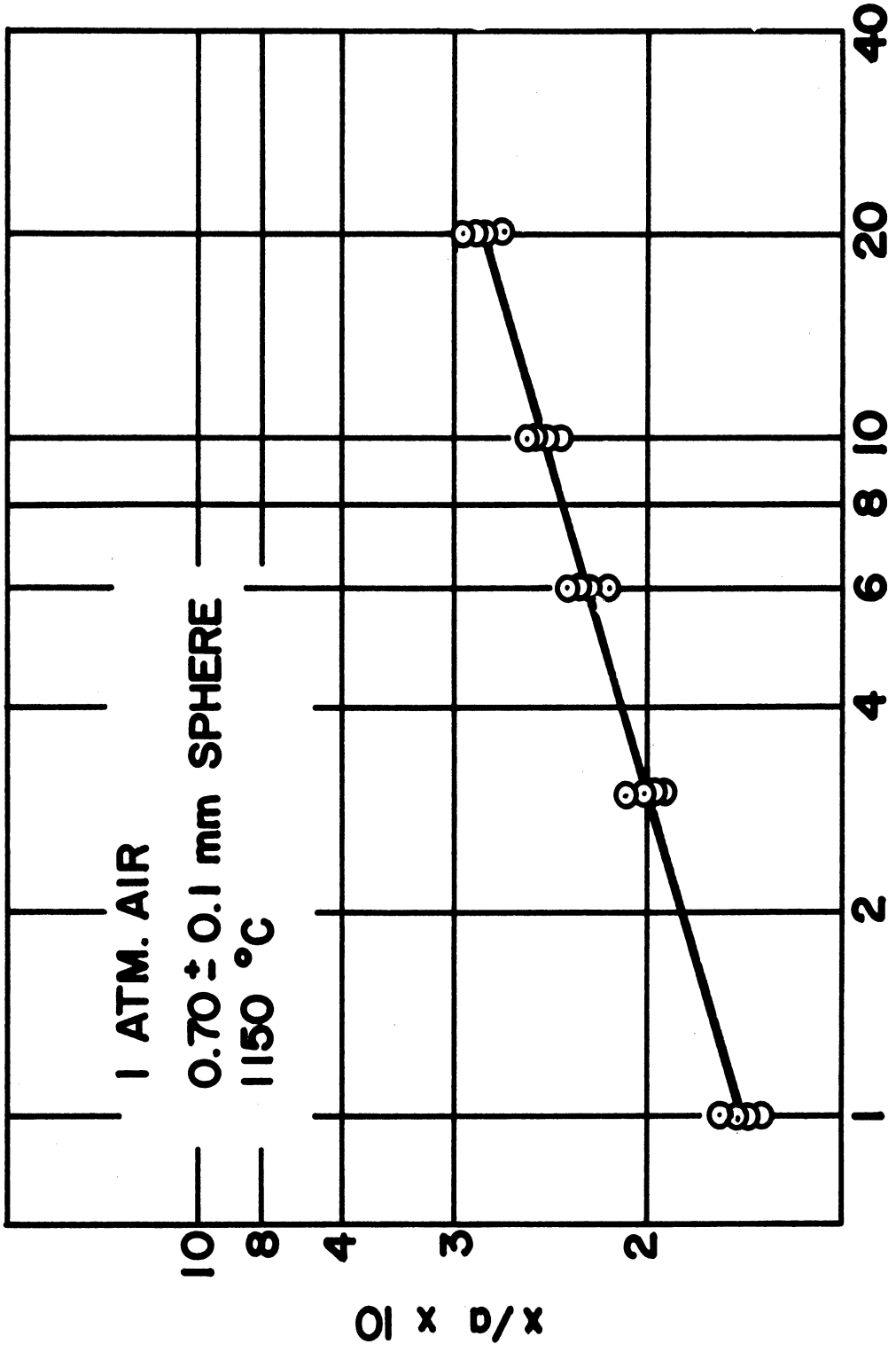

Fig. 2. Sintering of zinc oxide microspheres: neck width vs. time.

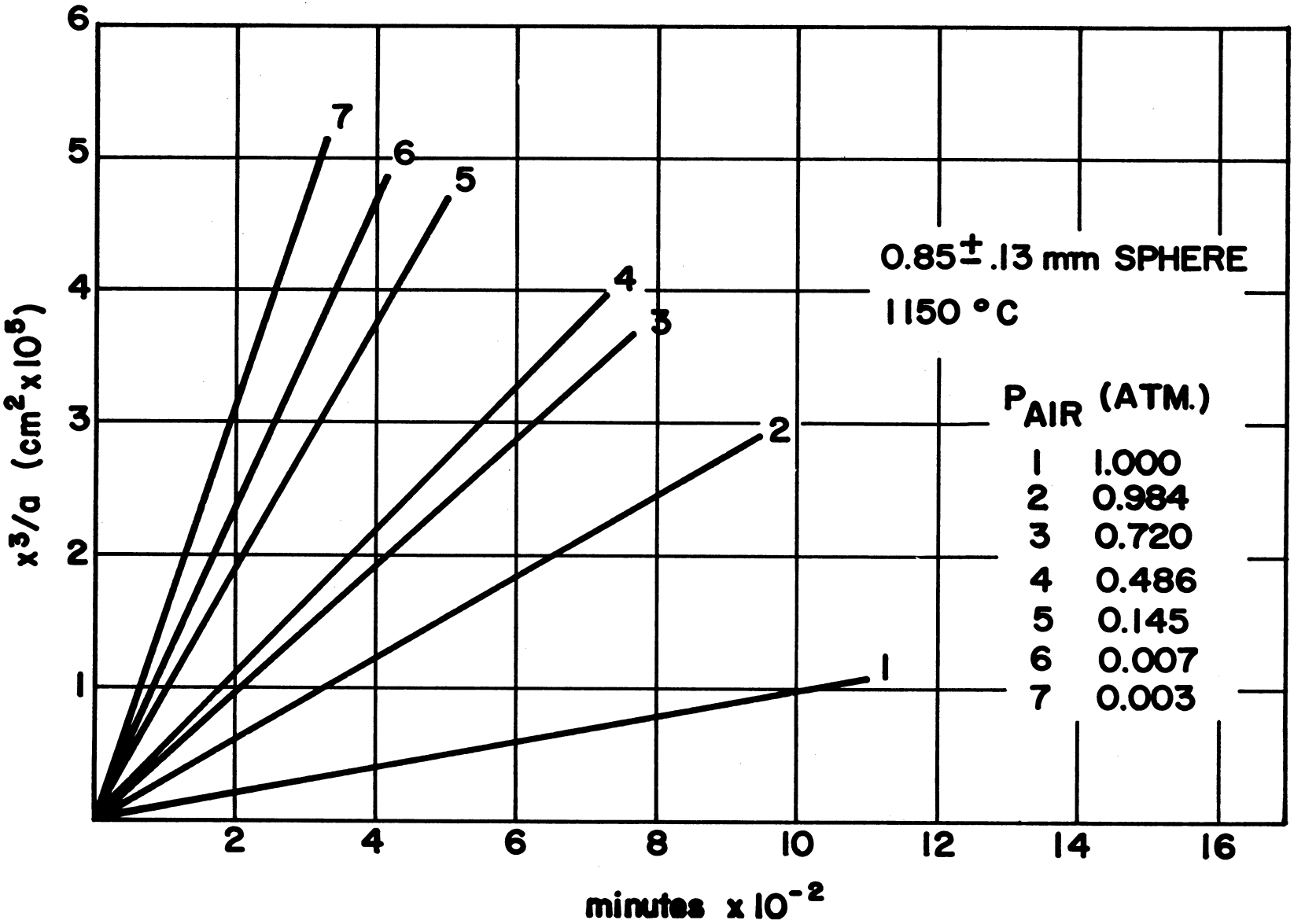

Fig. 3. Effect of total gas pressure on the sintering of zinc oxide: x, a, diameter of neck and diameter of spheres, respectively.

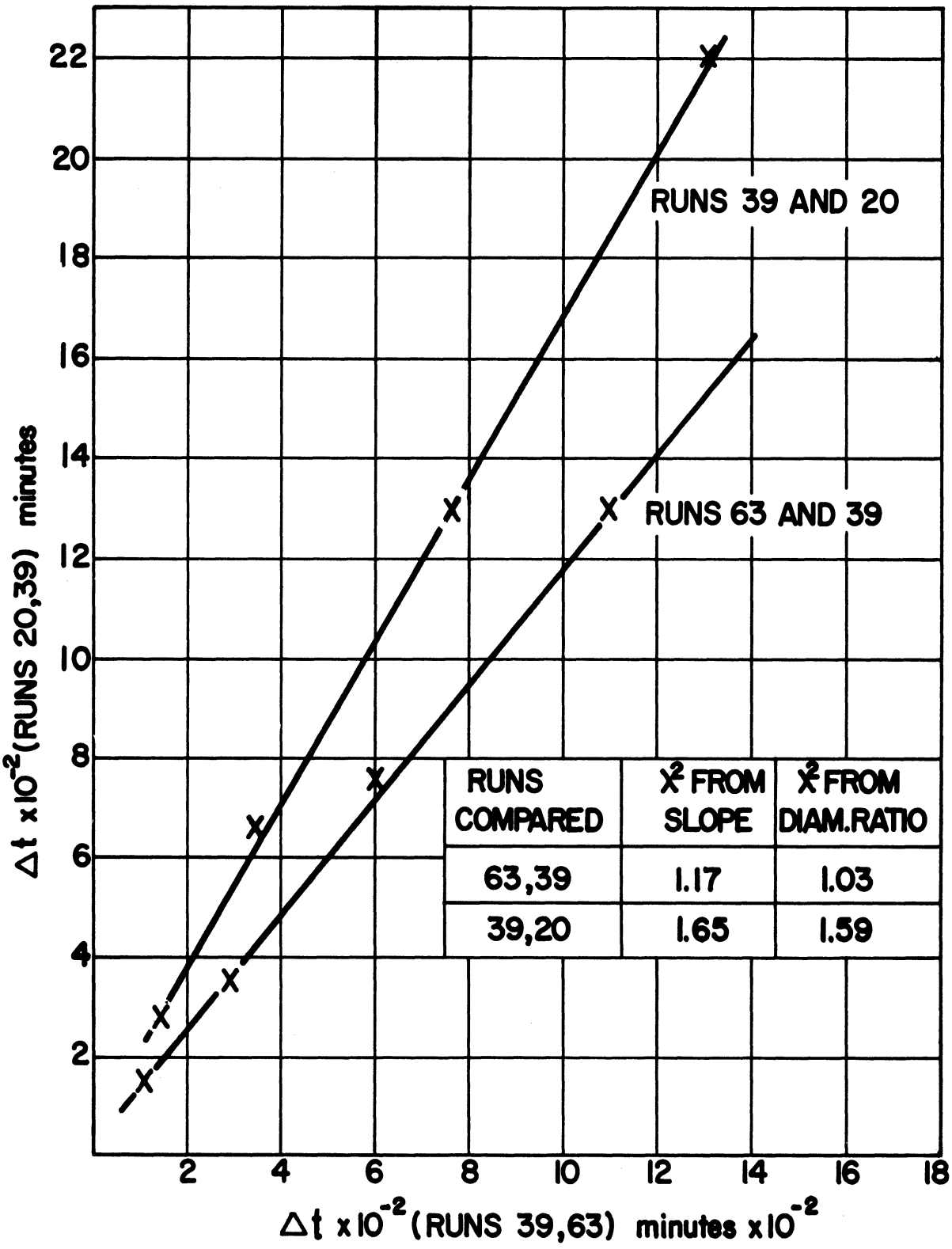

Fig. 4. Comparison between sphere size and sintering time for equivalent amount of neck growth during sintering of zinc oxide microspheres.

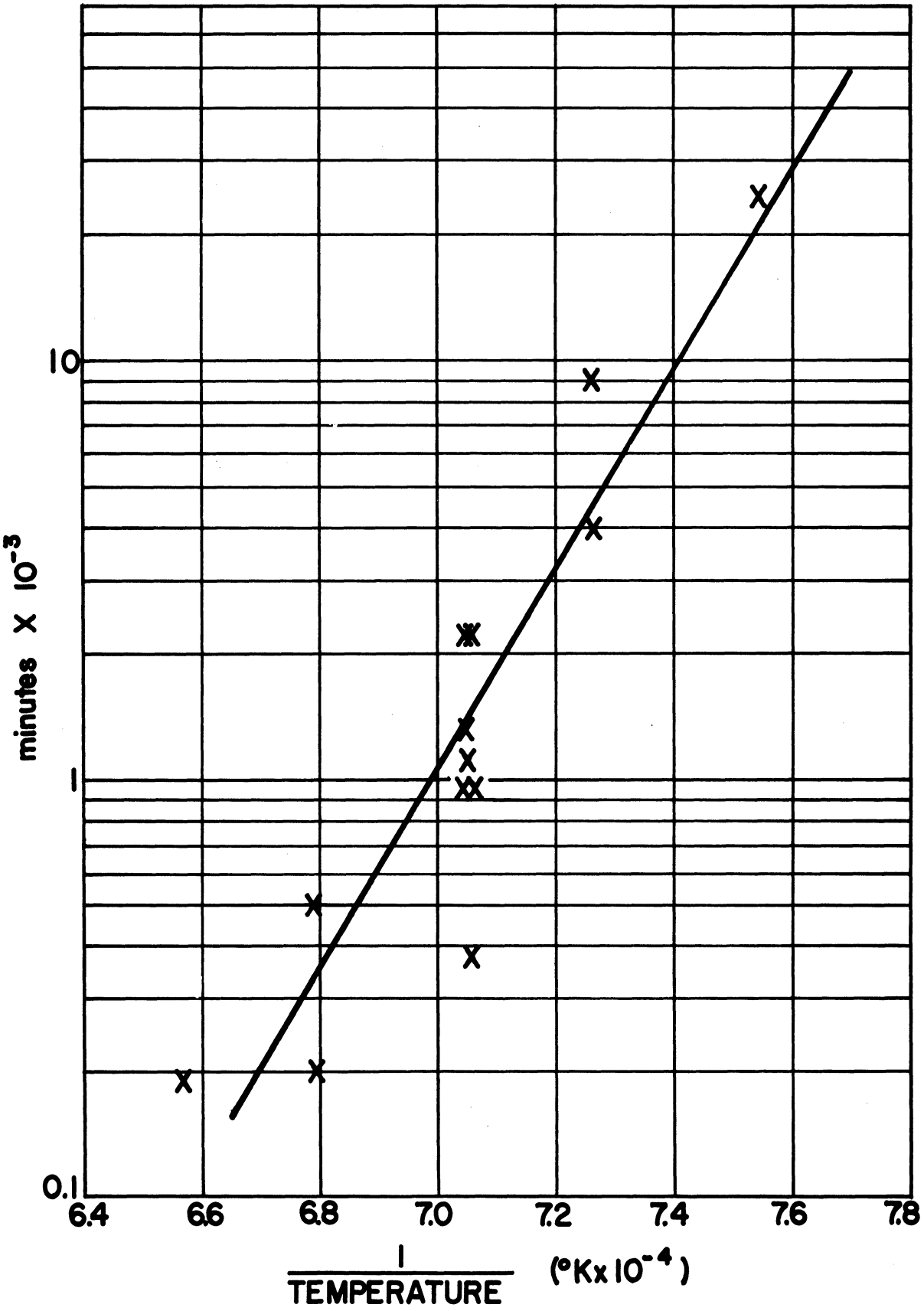

Fig. 5. Activation energy for sintering of zinc oxide microspheres, calculated from time to extent of sintering of 0.3.

DISTRIBUTION LIST

(One copy unless otherwise noted)

Air Force Office of Scientific
Research
Washington 25, D.C.
Attn: Solid State Sciences Division 3
Attn: Technical Library (SRGL) 2

ASTIA 10
Arlington Hall Station
Arlington 12, Virginia
Attn: TIPCR

Commander 2
Army Rocket & Guided Missile Agency
Redstone Arsenal, Alabama
Attn: ORDXR-OTL

RAND Corporation 2
1700 Main Street
Santa Monica, California

ARDC
Andrews Air Force Base
Washington 25, D.C.
Attn: RDRS

EOAFRD, ARDC
47 Cantersteen
Brussels, Belgium

HQ, USAF
Washington 25, D.C.
Attn: AFDRT

ARL
Building 450
Wright-Patterson Air Force Base
Ohio
Attn: Technical Library

WADD
Wright-Patterson Air Force Base
Ohio
Attn: WWAD

WADD
Materials Central
Wright-Patterson Air Force Base, Ohio
Attn: Metals & Ceramics Lab.
Attn: Physics Lab.
Attn: Materials Information Branch

Institute of Technology Library
MCLI-LIB, Building 125, Area B
Wright-Patterson Air Force Base, Ohio
Attn: AU

ARL
AFRD
Wright-Patterson Air Force Base, Ohio
Attn: Metallurgy
Attn: Solid State Physics

AFOSR
Holloman Air Force Base, New Mexico
Attn: SRLTL

AFCRL
L. G. Hanscom Field, Bedford, Mass.
Attn: CRRELA

AFFTC
Edwards Air Force Base, California
Attn: FTCTL

AEDC
Arnold Air Force Station, Tennessee
Attn: AEOIM

AFSWC
Kirtland Air Force Base, New Mexico
Attn: SWOI

Office of the Chief of Research
and Development
Department of the Army
Washington 25, D.C.
Attn: Scientific Information

Army Research Office
Box CM, Duke Station
Durham, North Carolina
Attn: CRD-AA-IP

Commanding Officer
Ordnance Materials Research Office
Watertown Arsenal
Watertown 72, Massachusetts
Attn: PS&C Div.

Commanding Officer
Watertown Arsenal Laboratories
Watertown 72, Massachusetts
Attn: Technical Reports Section

Commander
Signal Corps Engineering Laboratory
Fort Monmouth, New Jersey
Attn: SIGFM/EL-RPO

Director
U. S. Naval Research Laboratory
Washington 25, D.C.
Attn: Library

Department of the Navy
Office of Naval Research
Washington 25, D.C.
Attn: Code 423
Attn: Code 421

Officer in Charge
Office of Naval Research
Navy No. 100
Fleet Post Office
New York, New York

Commanding Officer
Naval Radiological Defense
Laboratory
San Francisco Naval Shipyard
San Francisco 24, California

Dr. D. F. Bleil
Associate Technical Director for
Research
U. S. Naval Ordnance Laboratory
White Oak, Silver Spring, Maryland

National Aeronautics & Space Agency
1520 H Street, N.W.
Washington 25, D.C.
Attn: Library

Ames Research Center (NASA)
Moffett Field, California
Attn: Technical Library

High Speed Flight Station (NASA)
Edwards Air Force Base, California
Attn: Technical Library

Langley Research Center (NASA)
Langley Air Force Base, Virginia
Attn: Technical Library

Lewis Research Center (NASA)
21000 Brookpark Road
Cleveland 35, Ohio
Attn: Technical Library

Wallops Station (NASA)
Wallops Island, Virginia
Attn: Technical Library

Division of Research
U.S. Atomic Energy Commission
Division Office
Washington 25, D.C.

U.S. Atomic Energy Commission
Library Branch
Technical Information Division, ORE
P. O. Box E
Oak Ridge, Tennessee

DISTRIBUTION LIST (Concluded)

Major John Radcliffe
ANP Office
U.S. Atomic Energy Commission
Washington 25, D.C.

Oak Ridge National Laboratory
P. O. Box P
Oak Ridge, Tennessee
Attn: Central Files

Brookhaven National Laboratory
Upton, Long Island, New York
Attn: Research Laboratory

Argonne National Laboratory
9700 S. Cass Avenue
Argonne, Illinois
Attn: Library

Document Custodian
Los Alamos Scientific Laboratory
P. O. Box 1663
Los Alamos, New Mexico

Ames Laboratory
Iowa State College
P. O. Box 14A, Station A
Ames, Iowa

Knolls Atomic Power Laboratory
P. O. Box 1072
Schenectady, New York
Attn: Document Librarian

National Science Foundation
1901 Constitution Avenue, N.W.
Washington 25, D.C.

National Bureau of Standards Library
Room 203, Northwest Building
Washington 25, D.C.

Director
Office of Technical Services
Department of Commerce
Technical Reports Branch
Washington 25, D.C.

Chairman
Canadian Joint Staff
2450 Massachusetts Avenue, N.W.
Washington, D.C.
Attn: DRB/DSIS

Defense Research Member
Canadian Joint Staff
Director of Engineering Research
Defense Research Board
Ottawa, Canada
Attn: Mr. H. C. Oatway

Institute of the Aeronautical Sciences
2 East 64th Street
New York 21, New York
Attn: Librarian